

Rif1 Prevents Resection of DNA Breaks and Promotes Immunoglobulin Class Switching

Michela Di Virgilio,¹ Elsa Callen,^{3*} Arito Yamane,^{4*} Wenzhu Zhang,^{5*} Mila Jankovic,¹ Alexander D. Gitlin,¹ Niklas Feldhahn,¹ Wolfgang Resch,⁴ Thiago Y. Oliveira,^{1,6,7} Brian T. Chait,⁵ André Nussenzweig,³ Rafael Casellas,⁴ Davide F. Robbiani,¹ Michel C. Nussenzweig^{1,2†}

¹Laboratory of Molecular Immunology, The Rockefeller University, New York, NY 10065, USA. ²Howard Hughes Medical Institute, The Rockefeller University, New York, NY 10065, USA. ³Laboratory of Genome Integrity and Center for Cancer Research, NCI, National Institutes of Health, Bethesda, MD 20892, USA.

⁴Genomics & Immunity and NIAMS, NCI, National Institutes of Health, Bethesda, MD 20892, USA.

⁵Laboratory of Mass Spectrometry and Gaseous Ion Chemistry, The Rockefeller University, New York, NY 10065, USA. ⁶Department of Genetics, Faculty of Medicine, University of São Paulo, Ribeirão Preto, Brazil.

⁷National Institute of Science and Technology for Stem Cells and Cell, Ribeirão Preto, Brazil.

*These authors contributed equally to this work.

†To whom correspondence should be addressed. E-mail: nussen@rockefeller.edu

DNA double-strand breaks (DSBs) represent a threat to the genome because they can lead to loss of genetic information and chromosome rearrangements. The DNA repair protein p53 binding protein 1 (53BP1) protects the genome by limiting nucleolytic processing of DSBs by a mechanism that requires its phosphorylation, but whether it does so directly is not known. Here we identify Rap1-interacting factor 1 (Rif1) as an Ataxia-Telangiectasia Mutated (ATM) phosphorylation-dependent interactor of 53BP1, and show that absence of Rif1 results in 5'-3' DNA end resection in mice. Consistent with enhanced DNA resection, Rif1 deficiency impairs DNA repair in the G1 and S phases of the cell cycle, interferes with class switch recombination (CSR) in B lymphocytes, and leads to accumulation of chromosome DSBs.

53BP1 is a multi-domain DNA damage response factor containing a chromatin-binding tudor domain, an oligomerization domain, tandem BRCA1 C-terminal (BRCT) domains, and an N-terminal domain with 28 SQ/TQ potential phosphorylation sites for phosphatidylinositol 3-kinase-related kinases [PIKKs, ATM/ATM and Rad3-related (ATR)/DNA-dependent protein kinase catalytic subunit (DNA-PKcs)] (1–3). 53BP1 contributes to DNA repair in several ways: it facilitates joining between intrachromosomal DSBs at a distance (synapsis) (4–7); it enables heterochromatic DNA repair through relaxation of nucleosome compaction (2, 3), and it protects DNA ends from resection and thereby favors repair of DSBs that occur in G1 by non-homologous end joining (NHEJ) (4, 5, 8). Consistent with its role in DNA end protection, 53BP1 is essential for CSR in B lymphocytes (9, 10).

Structure-function studies indicate that, besides its recruitment to DNA ends, protection requires 53BP1 phosphorylation (4), but how this protective effect is mediated is unknown. To identify phosphorylation-dependent interactors of 53BP1, we applied SILAC (Stable Isotope Labeling by Amino acids in Cell culture). *Trp53bp1^{-/-}* (*Trp53bp1* encodes 53BP1) B cells were infected with retroviruses encoding a C-terminal deleted version of 53BP1 (53BP1^{DB}) or a phosphomutant in which all 28 N-terminal potential PIKK phosphorylation sites were mutated to alanine (53BP1^{DB28A}) (4), in media containing isotopically heavy (53BP1^{DB}) or light (53BP1^{DB28A}) lysine and arginine (fig. S1, A to C) (11).

Most proteins co-precipitating with 53BP1^{DB} and 53BP1^{DB28A} displayed a H/(H + L) ratio of ~0.5, which is characteristic of phospho-

independent association (average of 0.57 ± 0.09 , peptide count ≥ 4) (Fig. 1 and table S1). Many of these proteins are non-specific contaminants, but others such as KRAB-associated protein 1 (KAP-1), dynein light chain LC8-type 1 (Dynll1), Nijmegen breakage syndrome 1 (Nbs1), and H2AX, represent authentic phospho-independent 53BP1 interacting proteins (fig. S1D). Three proteins displayed an abundance ratio that was more than four standard deviations above the mean indicating that they interact specifically with phosphorylated 53BP1: Pax interaction with transcription-activation domain protein-1 (Paxip1, or PTIP; 0.95), PTIP associated protein 1 (Pa1; 0.97), and Rif1 (0.96) (Fig. 1 and figs. S1D and S2). PTIP was known to interact with 53BP1 in a phospho-dependent manner (12) whereas Pa1 and Rif1 were not.

Rif1 was originally identified in budding yeast as a protein with a key role in telomere length maintenance (13). However, in mammalian cells, Rif1 is not essential for telomere homeostasis, but has been assigned a number of different roles in maintaining genome stability including participation in the DNA damage response (14–16), repair of S-phase DNA damage (17, 18), and regulation of origin firing during DNA replication (19, 20). However, the mechanism by which Rif1 might contribute to DNA repair

and maintaining genome stability is not known.

To confirm that Rif1 interaction with 53BP1 is phosphorylation dependent, we performed Western blot analysis of Flag-immunoprecipitates from lysates of irradiated *Trp53bp1^{-/-}* B cells infected with retroviruses encoding 53BP1^{DB} or 53BP1^{DB28A}. Whereas Dynll1, a phospho-independent 53BP1 interactor (SILAC ratio: 0.55) (fig. S1D), co-immunoprecipitated with 53BP1^{DB} and 53BP1^{DB28A} to a similar extent (Fig. 2A), only 53BP1^{DB} co-immunoprecipitated with Rif1. We conclude that the interaction between 53BP1 and Rif1 is dependent on phosphorylation of 53BP1.

ATM phosphorylates 53BP1 in response to irradiation-induced DSBs (1, 3). To determine whether ATM induces irradiation-dependent association between Rif1 and 53BP1, we compared irradiated and non-irradiated B cells in co-immunoprecipitation experiments. Although small amounts of Rif1 were detected in 53BP1^{DB} immunoprecipitates from unirradiated cells, this was increased by a factor higher than 3 after irradiation, and the increase was abrogated by treatment with the ATM inhibitor KU55933 (Fig. 2B). We conclude that Rif1 preferentially interacts with phosphorylated 53BP1 in a DNA damage- and ATM-dependent manner.

Rif1 is recruited to DNA damage foci by 53BP1 (15). To determine whether 53BP1 phosphorylation is required for Rif1 focus formation, we tested Rif1 foci in irradiated *Trp53bp1^{-/-}* immortalized mouse embryonic fibroblasts (iMEFs), which were stably transduced with either 53BP1^{DB} or 53BP1^{DB28A}. Rif1 foci were readily detected and co-localized with 53BP1^{DB} (Fig. 2C). In contrast, although 53BP1^{DB28A}

formed normal appearing foci, there were only rare Rifl foci that did not co-localize with 53BP1^{DB28A} (Fig. 2C). Furthermore, Rifl recruitment to ionizing radiation-induced foci (IRIF) and co-localization with 53BP1 was abrogated in ATM-deficient but not DNA-PKcs-deficient iMEFs (fig. S3) (15). We conclude that Rifl recruitment to DNA damage response foci is dependent on ATM-mediated 53BP1 phosphorylation.

53BP1 phosphorylation is essential for CSR (4). To examine the role of Rifl in joining DSBs during CSR, we conditionally ablated Rifl in B cells using CD19^{Cre}, which is expressed specifically in B cells (*Rifl*^{F/F}*Cd19*^{Cre/+} mice) (fig. S4, A to C). To induce CSR, B cells were activated with lipopolysaccharide (LPS) and interleukin (IL)-4 in vitro, and switching to IgG1 or IgG3 was measured by flow cytometry. CSR to IgG1 and IgG3 was markedly reduced in *Rifl*^{F/F}*Cd19*^{Cre/+} B cells, but less so than *Trp53bp1*^{-/-} controls (Fig. 3, A and B, and fig. S5). Switch junctions from *Rifl*^{F/F}*Cd19*^{Cre/+} B cells were comparable to *Trp53bp1*^{-/-} and wild type controls (7) (fig. S6), which indicates that, similar to 53BP1 deficiency, absence of Rifl does not alter the nature of productive CSR joining events. A similar CSR defect was also obtained by conditionally deleting Rifl with 4-hydroxy-tamoxifen (4HT) in *Rifl*^{F/F}*ROSA26*^{Cre-ERT2/+} B cells (fig. S7). Finally, shRNA-mediated partial down-regulation of CtBP-interacting protein (CtIP), which interacts with Rifl (fig. S8C), and has been implicated in processing of DNA ends (21, 22), resulted in a very small but reproducible increase in CSR (fig. S8, A and B). Thus, Rifl is essential for normal CSR, and CtIP may not be the only factor that contributes to end processing in Rifl-deficient B cells.

CSR requires cell division, activation-induced cytidine deaminase (AID) expression and *Igh* germline transcription (23). There are conflicting reports that Rifl is required for proliferation in MEFs, but not DT40 B cells (17, 18). We found that cell division profiles of *Rifl*^{F/F}*Cd19*^{Cre/+} and 4HT-treated *Rifl*^{F/F}*ROSA26*^{Cre-ERT2/+} B cells were indistinguishable from controls (Fig. 3, A and B; and fig. S7, A, C, E, and G), indicating that Rifl is dispensable for B cell proliferation in vitro. Finally, AID mRNA and protein expression, and *Igh* germline transcription were unaffected by Rifl deletion (fig. S4, B and D).

We next examined the role of Rifl in cell cycle progression in primary B cells. We found no major differences in the percentage of cells in G0/G1 and S-phases (Fig. 3C). However, the number of cells in G2/M was increased approximately twofold in the absence of Rifl (2.64, 2.56 and 1.91 fold at 48, 72, and 96 hours respectively) (Fig. 3C). Similar results were also obtained using *Rifl*^{F/F}*ROSA26*^{Cre-ERT2/+} B cells treated with 4HT (fig. S7, H and I). Furthermore, irradiation increases the accumulation of *Rifl*^{F/F}*Cd19*^{Cre/+} B cells in G2/M (Fig. 3D). In addition, *Trp53bp1*^{-/-} iMEFs expressing 53BP1^{DB28A}, which did not recruit Rifl to IRIF (Fig. 2C), exhibited delayed progression through S-phase following DNA damage with accumulation of cells in G2 after irradiation (fig. S9).

Accumulation of cells in G2/M may reflect the persistence of unrepaired DNA damage in a fraction of Rifl-deficient cells. To investigate this possibility, we analyzed metaphase spreads from B cells dividing in response to LPS and IL-4 in vitro. These cells express AID, which produces DSBs in *Igh*, and less frequently at off-target sites throughout the genome, in the G1 phase of the cell cycle (24–26). Chromosomal aberrations were increased in *Rifl*^{F/F}*Cd19*^{Cre/+} B cells compared to controls (Fig. 3E), with many localized to the *Igh* locus (Fig. 3E). Consistent with the observation that *Igh* is targeted by AID in the G1 phase of the cell cycle, all of the *Igh* breaks were chromosome breaks (Fig. 3, E and F). Interestingly, the frequency of *c-myc*/*Igh* translocations is moderately increased in *Rifl*^{F/F}*Cd19*^{Cre/+} B cells, however, the breakpoint distribution was similar to *Cd19*^{Cre/+} control (1.5×10^{-6} versus 1.0×10^{-6} in control, $P = 0.039$) (Fig. 3G and fig. S10). We conclude that in the absence of Rifl, DSBs fail to be resolved efficiently in the G1, S, or G2 phases leading to increased levels of genomic instability including

chromosome breaks at *Igh* and translocations in dividing B cells.

In the absence of 53BP1, DSBs produced by AID at the *Igh* locus accumulate the single-stranded DNA-binding replication protein A complex (RPA) as a result of increased DNA end resection (24). To determine if Rifl is required for DNA end protection by 53BP1, we performed RPA-ChIP-seq (chromatin immunoprecipitation followed by massive parallel sequencing) experiments on *Rifl*^{F/F}*Cd19*^{Cre/+} and control B cells. Ablation of Rifl was indistinguishable from loss of 53BP1 in that in its absence RPA decorates the *Igh* locus asymmetrically, in a manner consistent with 5'-3' resection (Fig. 4A) (27). In addition, absence of Rifl also results in RPA accumulation at non-*Igh* genes like *Il4ra* and *Pim1* that are damaged by AID in G1 (Fig. 4B) (24, 25). Rad51 is the recombinase that mediates repair of DSBs by homologous recombination in S/G2/M (22). To confirm that Rifl prevents resection that takes place in S-phase, we monitored Rad51 accumulation in activated B cells by ChIP-Seq. Loss of Rifl was indistinguishable from loss of 53BP1 (27), in that it led to asymmetric Rad51 accumulation at sites of AID-inflicted DNA damage (Fig. 4, C and D). We conclude that in the absence of Rifl, AID-induced DSBs incurred in G1 persist and undergo extensive 5'-3' DNA end resection in S/G2/M, as measured by RPA and Rad51 accumulation.

A role for Rifl in maintenance of genome stability and protection of DNA ends against resection is consistent with its phosphorylation-dependent recruitment to the N-terminal domain of 53BP1 (4). 53BP1 facilitates DNA repair and prevents DNA end resection during CSR. In the absence of 53BP1, AID-induced DSBs are resolved inefficiently in G1 leading to chromosome breaks, *Igh* instability, and resolution by alternative-NHEJ or HR instead of classical-NHEJ (4, 8, 27). Our experiments show that in the absence of Rifl, 53BP1 is insufficient to promote genomic stability, mediate efficient *Igh* repair, DNA end protection or CSR. Thus, these 53BP1 activities require Rifl recruitment to the phosphorylated N terminus of 53BP1. Rifl is likely to have additional functions beyond 53BP1, CSR and DNA end protection because whereas *Trp53bp1*^{-/-} mice are viable, Rifl deletion is lethal (17). Indeed, Rifl is believed to play a role in the repair of S-phase DNA damage (17, 18), and in the regulation of replication timing (19, 20, 28). Analogously, additional CSR factor(s) may exist downstream of 53BP1, as class switching in Rifl-deficient B cells is significantly higher than in *Trp53bp1*^{-/-}.

In summary our data are consistent with a model whereby ATM-mediated phosphorylation of 53BP1 recruits Rifl to sites of DNA damage, where it facilitates DNA repair in part by protecting DNA ends from resection (Fig. 4E). In the absence of Rifl, DNA breaks incurred in G1 fail to be repaired by NHEJ and undergo extensive 5'-3' end resection resulting in accumulation of chromosome breaks and genome instability.

References and Notes

1. M. M. Adams, P. B. Carpenter, Tying the loose ends together in DNA double strand break repair with 53BP1. *Cell Div.* **1**, 19 (2006). doi:10.1186/1747-1028-1-19 Medline
2. J. Lukas, C. Lukas, J. Bartek, More than just a focus: The chromatin response to DNA damage and its role in genome integrity maintenance. *Nat. Cell Biol.* **13**, 1161 (2011). doi:10.1038/ncb2344 Medline
3. A. T. Noon, A. A. Goodarzi, 53BP1-mediated DNA double strand break repair: Insert bad pun here. *DNA Repair (Amst.)* **10**, 1071 (2011). doi:10.1016/j.dnarep.2011.07.012 Medline
4. A. Bothmer *et al.*, Regulation of DNA end joining, resection, and immunoglobulin class switch recombination by 53BP1. *Mol. Cell* **42**, 319 (2011). doi:10.1016/j.molcel.2011.03.019 Medline
5. S. Difilippantonio *et al.*, 53BP1 facilitates long-range DNA end-joining during V(D)J recombination. *Nature* **456**, 529 (2008). doi:10.1038/nature07476 Medline

6. N. Dimitrova, Y. C. Chen, D. L. Spector, T. de Lange, 53BP1 promotes non-homologous end joining of telomeres by increasing chromatin mobility. *Nature* **456**, 524 (2008). doi:10.1038/nature07433 Medline
7. B. Reina-San-Martin, J. Chen, A. Nussenzweig, M. C. Nussenzweig, Enhanced intra-switch region recombination during immunoglobulin class switch recombination in 53BP1^{-/-} B cells. *Eur. J. Immunol.* **37**, 235 (2007). doi:10.1002/eji.200636789 Medline
8. A. Bothmer *et al.*, 53BP1 regulates DNA resection and the choice between classical and alternative end joining during class switch recombination. *J. Exp. Med.* **207**, 855 (2010). doi:10.1084/jem.20100244 Medline
9. J. P. Manis *et al.*, 53BP1 links DNA damage-response pathways to immunoglobulin heavy chain class-switch recombination. *Nat. Immunol.* **5**, 481 (2004). doi:10.1038/ni1067 Medline
10. I. M. Ward *et al.*, 53BP1 is required for class switch recombination. *J. Cell Biol.* **165**, 459 (2004). doi:10.1083/jcb.200403021 Medline
11. Materials and methods are available as supplementary materials on *Science* Online.
12. I. A. Manke, D. M. Lowery, A. Nguyen, M. B. Yaffe, BRCT repeats as phosphopeptide-binding modules involved in protein targeting. *Science* **302**, 636 (2003). doi:10.1126/science.108877 Medline
13. C. F. Hardy, L. Sussel, D. Shore, A RAP1-interacting protein involved in transcriptional silencing and telomere length regulation. *Genes Dev.* **6**, 801 (1992). doi:10.1101/gad.6.5.801 Medline
14. S. Kumar *et al.*, Role for Rif1 in the checkpoint response to damaged DNA in *Xenopus* egg extracts. *Cell Cycle* **11**, 1183 (2012). doi:10.4161/cc.11.6.19636 Medline
15. J. Silverman, H. Takai, S. B. Buonomo, F. Eisenhaber, T. de Lange, Human Rif1, ortholog of a yeast telomeric protein, is regulated by ATM and 53BP1 and functions in the S-phase checkpoint. *Genes Dev.* **18**, 2108 (2004). doi:10.1101/gad.1216004 Medline
16. L. Xu, E. H. Blackburn, Human Rif1 protein binds aberrant telomeres and aligns along anaphase midzone microtubules. *J. Cell Biol.* **167**, 819 (2004). doi:10.1083/jcb.200408181 Medline
17. S. B. Buonomo, Y. Wu, D. Ferguson, T. de Lange, Mammalian Rif1 contributes to replication stress survival and homology-directed repair. *J. Cell Biol.* **187**, 385 (2009). doi:10.1083/jcb.200902039 Medline
18. D. Xu *et al.*, Rif1 provides a new DNA-binding interface for the Bloom syndrome complex to maintain normal replication. *EMBO J.* **29**, 3140 (2010). doi:10.1038/emboj.2010.186 Medline
19. D. Cornacchia *et al.*, Mouse Rif1 is a key regulator of the replication-timing programme in mammalian cells. *EMBO J.* **31**, 3678 (2012). doi:10.1038/emboj.2012.214 Medline
20. S. Yamazaki *et al.*, Rif1 regulates the replication timing domains on the human genome. *EMBO J.* **31**, 3667 (2012). doi:10.1038/emboj.2012.180 Medline
21. A. A. Sartori *et al.*, Human CtIP promotes DNA end resection. *Nature* **450**, 509 (2007). doi:10.1038/nature06337 Medline
22. L. S. Symington, J. Gautier, Double-strand break end resection and repair pathway choice. *Annu. Rev. Genet.* **45**, 247 (2011). doi:10.1146/annurev-genet-110410-132435 Medline
23. R. Pavri, M. C. Nussenzweig, AID targeting in antibody diversity. *Adv. Immunol.* **110**, 1 (2011). doi:10.1016/B978-0-12-387663-8.00005-3 Medline
24. O. Hakim *et al.*, DNA damage defines sites of recurrent chromosomal translocations in B lymphocytes. *Nature* **484**, 69 (2012). Medline
25. S. Petersen *et al.*, AID is required to initiate Nbs1/γ-H2AX focus formation and mutations at sites of class switching. *Nature* **414**, 660 (2001). doi:10.1038/414660a Medline
26. A. Yamane *et al.*, Deep-sequencing identification of the genomic targets of the cytidine deaminase AID and its cofactor RPA in B lymphocytes. *Nat. Immunol.* **12**, 62 (2011). doi:10.1038/ni.1964 Medline
27. A. Yamane *et al.*, RPA accumulation during class switch recombination represents 5'-3' DNA end resection during the S-G2/M phase of the cell cycle. *Cell Rep.* 10.1016/j.celrep.2012.12.006 (2013).
28. M. Hayano *et al.*, Rif1 is a global regulator of timing of replication origin firing in fission yeast. *Genes Dev.* **26**, 137 (2012). doi:10.1101/gad.178491.111 Medline
29. C. de Luca *et al.*, Complete rescue of obesity, diabetes, and infertility in db/db mice by neuron-specific LEPR-B transgenes. *J. Clin. Invest.* **115**, 3484 (2005). doi:10.1172/JCI24059 Medline
30. R. C. Rickert, J. Roes, K. Rajewsky, B lymphocyte-specific, Cre-mediated mutagenesis in mice. *Nucleic Acids Res.* **25**, 1317 (1997). doi:10.1093/nar/25.6.1317 Medline
31. D. F. Robbiani *et al.*, AID is required for the chromosomal breaks in c-myc that lead to c-myc/IgH translocations. *Cell* **135**, 1028 (2008). doi:10.1016/j.cell.2008.09.062 Medline
32. I. M. Cristea *et al.*, Host factors associated with the Sindbis virus RNA-dependent RNA polymerase: Role for G3BP1 and G3BP2 in virus replication. *J. Virol.* **84**, 6720 (2010). doi:10.1128/JVI.01983-09 Medline
33. A. N. Krutchinsky, M. Kalkum, B. T. Chait, Automatic identification of proteins with a MALDI-quadrupole ion trap mass spectrometer. *Anal. Chem.* **73**, 5066 (2001). doi:10.1021/ac010682o Medline
34. J. Rappaport, M. Mann, Y. Ishihama, Protocol for micro-purification, enrichment, pre-fractionation and storage of peptides for proteomics using StageTips. *Nat. Protoc.* **2**, 1896 (2007). doi:10.1038/nprot.2007.261 Medline
35. J. Cox, M. Mann, MaxQuant enables high peptide identification rates, individualized p.p.b.-range mass accuracies and proteome-wide protein quantification. *Nat. Biotechnol.* **26**, 1367 (2008). doi:10.1038/nbt.1511 Medline
36. K. M. McBride, V. Barreto, A. R. Ramiro, P. Stavropoulos, M. C. Nussenzweig, Somatic hypermutation is limited by CRM1-dependent nuclear export of activation-induced deaminase. *J. Exp. Med.* **199**, 1235 (2004). doi:10.1084/jem.20040373 Medline
37. E. Callén *et al.*, Essential role for DNA-PKcs in DNA double-strand break repair and apoptosis in ATM-deficient lymphocytes. *Mol. Cell* **34**, 285 (2009). doi:10.1016/j.molcel.2009.04.025 Medline
38. M. Muramatsu *et al.*, Class switch recombination and hypermutation require activation-induced cytidine deaminase (AID), a potential RNA editing enzyme. *Cell* **102**, 553 (2000). doi:10.1016/S0092-8674(00)00078-7 Medline
39. R. Pavri *et al.*, Activation-induced cytidine deaminase targets DNA at sites of RNA polymerase II stalling by interaction with Spt5. *Cell* **143**, 122 (2010). doi:10.1016/j.cell.2010.09.017 Medline
40. B. Reina-San-Martin *et al.*, H2AX is required for recombination between immunoglobulin switch regions but not for intra-switch region recombination or somatic hypermutation. *J. Exp. Med.* **197**, 1767 (2003). doi:10.1084/jem.20030569 Medline
41. A. R. Ramiro *et al.*, Role of genomic instability and p53 in AID-induced c-myc-Igh translocations. *Nature* **440**, 105 (2006). doi:10.1038/nature04495 Medline
42. A. Valouev *et al.*, Genome-wide analysis of transcription factor binding sites based on ChIP-Seq data. *Nat. Methods* **5**, 829 (2008). doi:10.1038/nmeth.1246 Medline
43. E. Callén *et al.*, ATM prevents the persistence and propagation of chromosome breaks in lymphocytes. *Cell* **130**, 63 (2007). doi:10.1016/j.cell.2007.06.016 Medline
44. M. S. Huen *et al.*, Regulation of chromatin architecture by the PWWP domain-containing DNA damage-responsive factor EXPAND1/MUM1. *Mol. Cell* **37**, 854 (2010). doi:10.1016/j.molcel.2009.12.040 Medline
45. K. W.-H. Lo *et al.*, The 8-kDa dynein light chain binds to p53-binding protein 1 and mediates DNA damage-induced p53 nuclear accumulation. *J. Biol. Chem.* **280**, 8172 (2005). doi:10.1074/jbc.M411408200 Medline
46. I. Rappold, K. Iwabuchi, T. Date, J. Chen, Tumor suppressor p53 binding protein 1 (53BP1) is involved in DNA damage-signaling pathways. *J. Cell Biol.* **153**, 613 (2001). doi:10.1083/jcb.153.3.613 Medline
47. A. T. Noon *et al.*, 53BP1-dependent robust localized KAP-1 phosphorylation is essential for heterochromatic DNA double-strand break repair. *Nat. Cell Biol.* **12**, 177 (2010). doi:10.1038/ncb2017 Medline
48. F. M. Boisvert, A. Rhie, S. Richard, A. J. Doherty, The GAR motif of 53BP1 is arginine methylated by PRMT1 and is necessary for 53BP1 DNA binding activity. *Cell Cycle* **4**, 1834 (2005). doi:10.4161/cc.4.12.2250 Medline
49. K. Yamane, X. Wu, J. Chen, A DNA damage-regulated BRCT-containing protein, TopBP1, is required for cell survival. *Mol. Cell. Biol.* **22**, 555 (2002). doi:10.1128/MCB.22.2.555-566.2002 Medline

Acknowledgments: We thank all members of the Nussenzweig laboratory for discussion, D. Bosque and T. Eisenreich for help in managing mouse colonies, A. Gazumyan for assistance with *Igh* germline and AID transcript levels analysis, and K. Yao for help with genotyping. We thank T. de Lange (The Rockefeller University, New York) for Rif1^{F/F} mice, S. Buonomo (EMBL Mouse Biology Unit, Monterotondo) for the anti-mouse Rif1 serum

#1240, and G. Gutierrez (NIAMS, NIH, Bethesda) for Illumina sequencing. We are grateful to N. Zampieri (Columbia University, New York) for assistance with IF image processing and to M. P. Rout, J. LaCava, S. Obado, and L. Hough (The Rockefeller University, New York) for invaluable help, discussions, and protocols for cryolysis and magnetic bead-mediated immunoisolation. The data presented in the manuscript are tabulated in the main text and in the supplementary materials. Sequence data shown in Fig. 4 have been deposited in the Gene Expression Omnibus database at <http://www.ncbi.nlm.nih.gov/geo/>. M.D.V. was a Fellow of the American Italian Cancer Foundation. A.D.G. was supported by NIH MSTP grant GM007739. This work was supported in part by NIH grants AI037526 (M.C.N.), RR022220 (B.T.C.), RR00862 (B.T.C.), GM103314 (B.T.C.), and by the intramural program of NIAMS at the NIH (R.C.). M.C.N. is an HHMI Investigator.

Supplementary Materials

www.sciencemag.org/cgi/content/full/science.1230624/DC1

Materials and Methods

Figs. S1 to S10

Table S1

References (29–49)

24 September 2012; accepted 16 November 2012

Published online 10 January 2013

10.1126/science.1230624

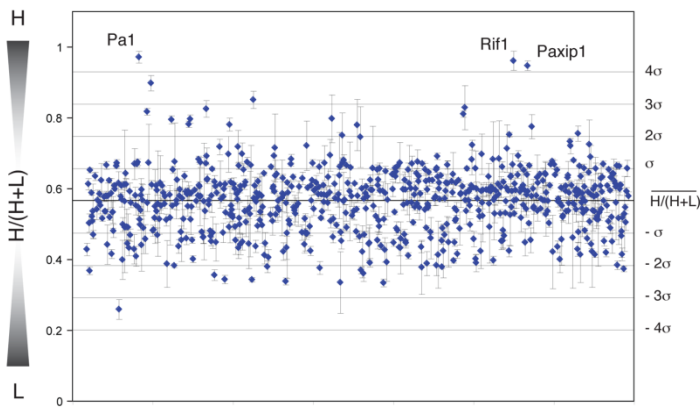


Fig. 1. Identification of phospho-dependent 53BP1 interactors. Graph shows the $H/(H + L)$ ratio distribution of proteins identified by SILAC. Error bars represent the standard deviation of the $H/(H + L)$ mean value for all the peptides identified for each individual protein (only proteins with ≥ 4 peptides were included). " $H/(H + L)$ " and " σ " are the mean (0.57) and SD (0.09) of the distribution, respectively. H: heavy; L: light.

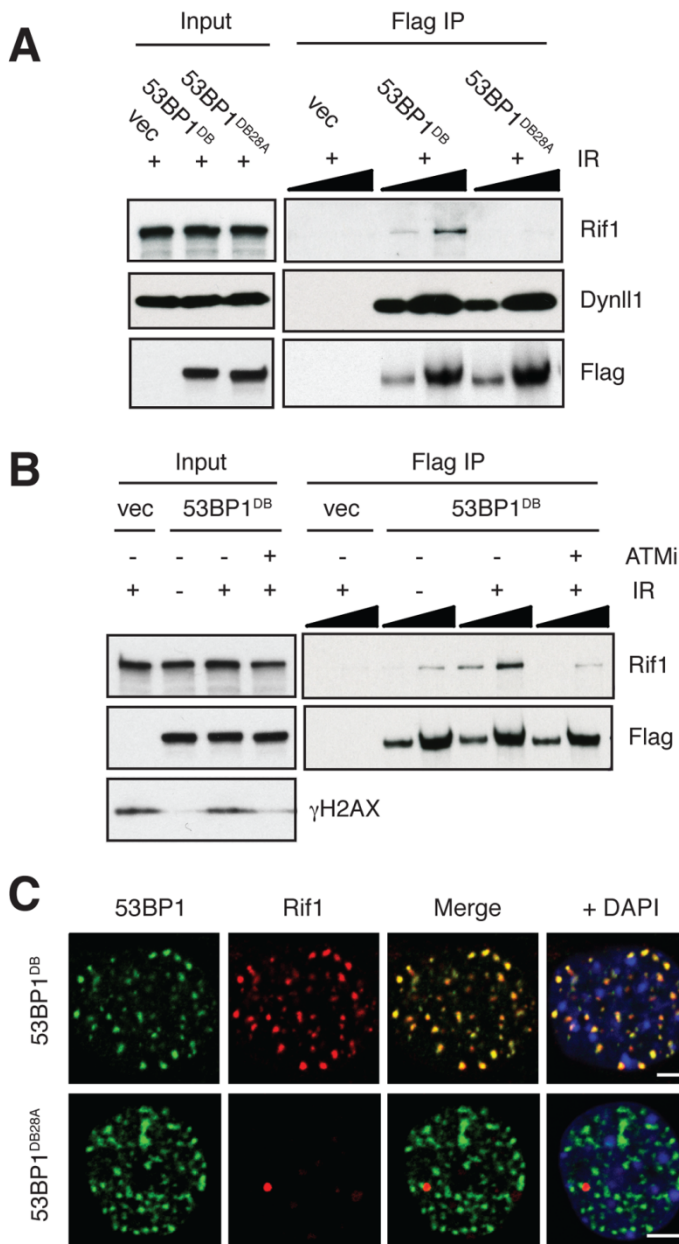


Fig. 2. Rif1 interaction with 53BP1 is phospho-, damage- and ATM-dependent. **(A)** Western blot analysis of anti-Flag immuno-precipitates from irradiated *Trp53bp1*^{-/-} B lymphocytes infected with empty vector (vec), 53BP1^{DB}, or 53BP1^{DB28A} virus. Triangles indicate 3-fold dilution. Data are representative of two independent experiments. **(B)** Western blot analysis of anti-Flag immunoprecipitates from *Trp53bp1*^{-/-} B cells infected with empty vector or 53BP1^{DB}. Cells were either left untreated or irradiated (50 Gy, 45 min recovery) in the presence or absence of the ATM kinase inhibitor KU55933 (ATMi). Triangles indicate 3-fold dilution. Data are representative of two independent experiments. **(C)** Immunofluorescent staining for 53BP1 (Flag) and Rif1 in irradiated *Trp53bp1*^{-/-} iMEFs reconstituted with 53BP1^{DB} or 53BP1^{DB28A} retroviruses (4). Magnification, 100X; Scale bars, 5 μ m. Data are representative of two independent experiments.

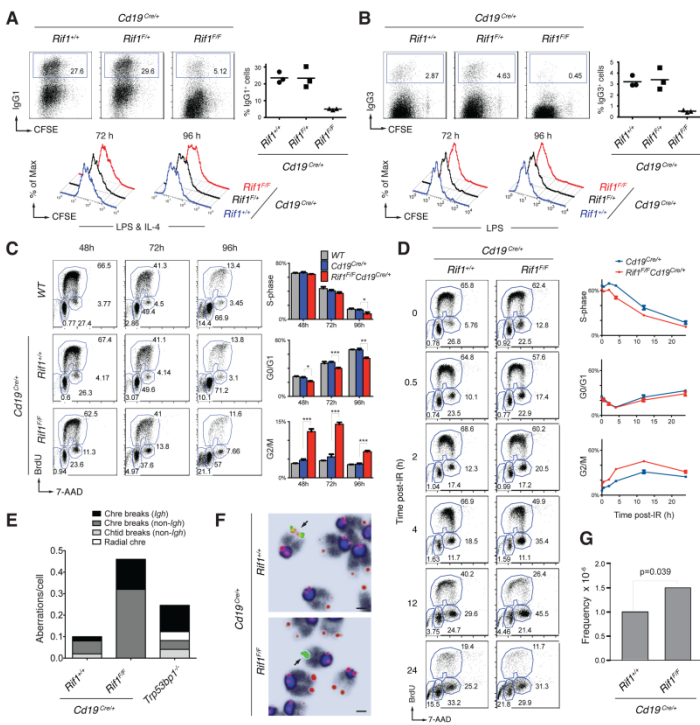


Fig. 3. Rif1 deficiency impairs class switch recombination, and causes *Igh* and genome instability in primary B cells. **(A)** (Left) CSR to IgG1 96 hours post-stimulation of B lymphocytes with LPS and IL-4. (Right) Summary dot plot for three independent experiments ($n = 3$ mice per genotype). Mean values are: 23.6% for *Cd19^{Cre/+}*, 23.4% for *Rif1^{F/F} Cd19^{Cre/+}*, and 5.0% for *Rif1^{F/F}* (*Cd19^{Cre/+}*) ($P < 0.008$ with the paired student's *t* test). (Bottom) B cell proliferation by carboxyfluorescein succinimidyl ester (CFSE) dilution. Data are representative of three independent experiments. **(B)** Same as in (A) but for CSR to IgG3 after stimulation with LPS alone. Mean values are: 3.2% for *Cd19^{Cre/+}*, 3.4% for *Rif1^{F/F} Cd19^{Cre/+}*, and 0.5% for *Rif1^{F/F}* (*Cd19^{Cre/+}*) ($P < 0.008$). **(C)** (Left) Cell cycle analysis of primary B cells after stimulation with LPS and IL-4. (Right) Summary histograms for S-phase, G0/G1 and G2/M cells from two independent experiments ($n = 4$ mice per genotype). Error bars indicate SEM. * $0.01 < P < 0.05$, ** $0.001 < P < 0.01$, *** $P < 0.001$. **(D)** (Left) Cell cycle analysis of LPS- and IL-4-stimulated splenocytes at the indicated times post-irradiation (6 Gy). (Right) Summary graphs for S-phase, G0/G1 and G2/M cells from two independent experiments ($n = 3$ mice per genotype). Error bars indicate SD. **(E)** Analysis of genomic instability in metaphases from B cell cultures. Chtid: chromatid; Chre: chromosome. Data are representative of two independent experiments ($n = 50$ metaphases analyzed per genotype per experiment). **(F)** Examples of *Igh*-associated aberrations in *Rif1^{F/F} Cd19^{Cre/+}* B cells. Chromosomes were hybridized with an *Igh* Ca probe (green; centromeric of Cy1) and a telomere sequence-specific probe (red), and counterstained with DAPI (dark blue/black). Magnification, 63X; Scale bars, 1 μm. **(G)** Frequency of *c-myc*/*Igh* translocations in activated B cells. Graph shows combined results from 3 mice per genotype.

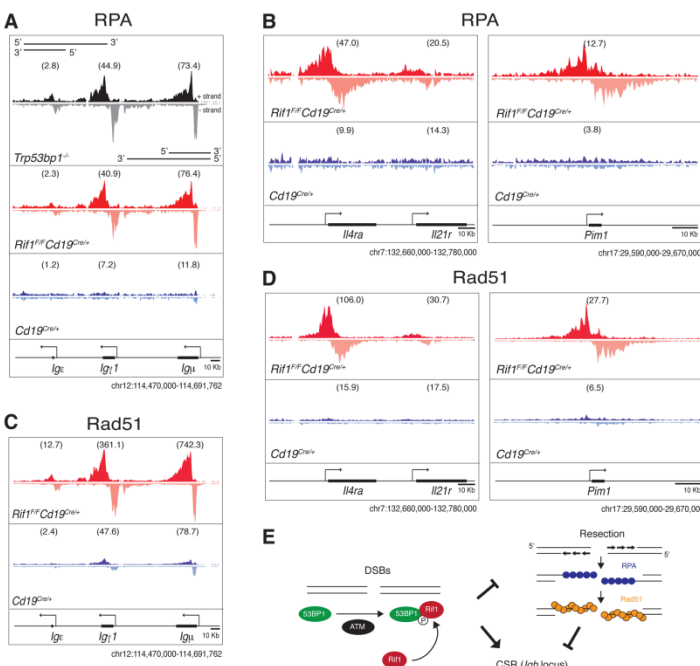


Fig. 4. Rif1 prevents resection of DNA ends at sites of AID-induced DNA damage. **(A) to (D)** RPA and Rad51 occupancy at the *Igh* locus (A and C) and at non-*Igh* AID target genes (B and D) in B cells activated to undergo class switching. ChIP-seq libraries were resolved into upper (+) and lower (-) DNA strands to show RPA and Rad51 association with sense and antisense strands. Within a specified genomic window, graphs have the same scale and show tag density. Deep-sequencing samples were normalized per library size, and TPM (Tags Per Million) values were calculated for each genomic region as indicated in Materials and Methods and shown in parenthesis. Data are representative of two independent experiments for RPA ChIP-seq and one for Rad51. **(E)** Model of Rif1 recruitment and DNA end protection at DSBs. DNA damage activates ATM, which phosphorylates many targets, including 53BP1. This event recruits Rif1 to 53BP1 at the DSB, where it inhibits DNA resection. The extensive resection in the absence of Rif1 impairs CSR at the *Igh* locus.